Available online at www.sciencedirect.com

ScienceDirect

Ceramics International 40 (2014) 557–562

CERAMICS INTERNATIONAL

www.elsevier.com/locate/ceramint

Relaxor behavior and energy storage performance of ferroelectric PLZT thin films with different Zr/Ti ratios☆

Zhongqiang Hu*, Beihai Ma, Shanshan Liu, Manoj Narayanan, Uthamalingam Balachandran

Energy Systems Division, Argonne National Laboratory, Argonne, IL 60439, USA

Received 18 April 2013; received in revised form 23 May 2013; accepted 24 May 2013
Available online 18 June 2013

Abstract

Ferroelectric lead lanthanum zirconate titanate (PLZT) films with 8 mol% lanthanum and different Zr/Ti ratios (70/30, 65/35, 58/42, 52/48, 45/55, and 40/60) have been grown on platinized silicon substrates by chemical solution deposition. The effects of the Zr/Ti ratios on the dielectric and ferroelectric properties were investigated for high-power energy storage applications. These films exhibited relaxor behavior and slim polarization–electric field hysteresis loops, and the degree of phase transition diffuseness decreased with increasing Ti. The PLZT films with Zr/Ti = 52/48 had a high spontaneous polarization of ≈51.2 μC/cm^2, a low remanent polarization of ≈9.1 μC/cm^2, and a low coercive electric field of ≈25.9 kV/cm, leading to a recoverable energy density of ≈30 J/cm^3 and a charge–discharge efficiency of ≈78% at room temperature. The high energy density and high efficiency indicate that relaxor PLZT with La/Zr/Ti = 8/52/48 is a promising candidate for high-power film capacitors.

Keywords: A. Sol–gel processes; C. Ferroelectric properties; D. PLZT; E. Capacitors

1. Introduction

Ceramic film capacitors have recently attracted considerable interest for short-term energy storage in renewable energy systems such as wind turbines and electric vehicles, due to their high dielectric constant and reliability compared to polymer and electrolyte capacitors [1–6]. The ceramic materials used for capacitors can be paraelectric (linear dielectric), normal ferroelectric, antiferroelectric, or relaxor ferroelectric [3–8]. In a capacitor, when the electric field E increases from zero to the maximum E_m, the polarization P increases to P_m, and electric energy is stored in the capacitor. The energy stored per unit volume is defined by $U_{\mathrm{st}} = \int_0^{P_m} E\, dP$. As the electric field decreases from E_m to zero, the stored energy is released on discharge from P_m to remanent polarization P_r. The recoverable electric energy density U_{re} is then represented as $U_{\mathrm{re}} = \int_{P_r}^{P_m} E\, dP$. The charge–discharge efficiency η can then be calculated by $\eta = (U_{re}/U_{st}) \times 100\%$. To minimize the size and weight of capacitors, ceramic films with high U_{re} and high η are required. From the polarization–electric field (P–E) hysteresis loops of ceramic materials, it is clear that lower P_r and higher P_m lead to higher recoverable energy density at fixed E_m. One can also conclude that linear dielectrics exhibit the highest efficiency for energy storage because of their low energy loss ($U_{st} \approx U_{re}$); however, the low P_m in linear dielectrics depresses the energy density [9–11]. Normal ferroelectrics exhibit relatively high P_r and large coercive electric field (E_c), leading to low energy density and efficiency [10]. Antiferroelectrics have low P_r and E_c but also wide hysteresis loops, contributing to large energy loss [12–16]. In contrast, relaxor ferroelectrics exhibit slim P–E hysteresis loops with high P_m and low P_r and E_c, implying higher energy storage density and better energy conversion efficiency [8].

☆The submitted manuscript has been created by UChicago Argonne, LLC, Operator of Argonne National Laboratory ("Argonne"). Argonne, a US Department of Energy Office of Science laboratory, is operated under Contract No. DE-AC02-06CH11357. The US Government retains for itself, and others acting on its behalf, a paid-up nonexclusive, irrevocable worldwide license in said article to reproduce, prepare derivative works, distribute copies to the public, and perform publicly and display publicly, by or on behalf of the Government.

*Corresponding author. Tel.: +1 630 252 4193; fax: +1 630 252 3604.
E-mail address: zqhu@anl.gov (Z. Hu).

0272-8842/$ - see front matter © 2013 Elsevier Ltd and Techna Group S.r.l. All rights reserved.
http://dx.doi.org/10.1016/j.ceramint.2013.05.139

Lead lanthanum zirconate titanate (PLZT) films are considered as one of the most promising candidates for high-power energy storage [12]. Generally, when PLZT has a high concentration of lanthanum (≥7 mol%), the c/a ratio of the unit cell decreases to near unity, approaching a pseudocubic structure. This condition leads to relaxor behavior and slim *P–E* hysteresis loops [7,8]. Several research groups have reported investigations on PLZT-based relaxor ferroelectrics for energy storage applications [17–21]. Sigman et al. reported a recoverable energy density of ≈22 J/cm^3 in PLZT (12/70/30) thin films deposited on platinized silicon (PtSi) [19]. Kim et al. observed a high capacitance density of ≈2.4 μF/cm^2 in PLZT (7/62/38) thin films deposited on nickel with a lanthanum nickel oxide buffer (LNO/Ni) [20]. Hao et al. studied PLZT (9/65/35) films on PtSi and reported a high recoverable energy density of ≈28.7 J/cm^3 and an energy efficiency of ≈60% [21]. Recently, PLZT (8/52/48) films have received increasing interest due to their excellent ferroelectric and dielectric properties and high Curie temperature [6,13,22]. Energy-storage densities of ≈13 and 45 J/cm^3 have been reported in PLZT (8/52/48) films deposited on PtSi and LNO/Ni, respectively [10,13]. These reports demonstrated the possibility of using PLZT relaxor ferroelectrics for high-power energy storage. However, the relationship between the composition and the energy storage capability has not been studied in relaxor PLZT. In this work, we systematically investigated the effects of the Zr/Ti ratio on the relaxor behavior and energy storage performance of PLZT film capacitors grown on PtSi.

2. Experimental procedures

PLZT precursor solutions (0.5 M) with various Zr/Ti ratios (Zr/Ti=70/30, 65/35, 58/42, 52/48, 45/55, and 40/60) were prepared by a modified 2-methoxyethanol synthesis route. In the solutions, 8 mol% lanthanum was added to enhance the relaxor behavior and insulating property [2]. The starting chemicals were lead acetate trihydrate, lanthanum nitrate hexahydrate, zirconium propoxide, and titanium isopropoxide. Excess lead (20 mol%) was used to compensate for the lead loss during the high temperature crystallization. Detailed solution synthesis conditions can be found in our prior report [6]. The PLZT films were grown by spin coating the solution on PtSi substrates at 3000 rpm for 30 s. Each layer was pyrolyzed at 450 °C for 10 min before being annealed at 650 °C for 5 min. An additional annealing at 650 °C for 5 min was applied after every three layers of coating. A final crystallization anneal was performed at 650 °C for 15 min. The thickness of the PLZT films with six layers of coating was ≈690 nm, resulting in a per-coating thickness of ≈115 nm. Platinum top electrodes with a diameter of 250 μm and a thickness of 100 nm were deposited on the prepared samples through a shadow mask by electron-beam evaporation.

Phase identification was carried out by analysis using a Bruker D8 AXS diffractometer with General Area Detector Diffraction System. A Signatone QuieTemp® probe station with heatable vacuum chuck (Lucas Signatone Corp., Gilroy, CA) was used for electrical characterization. Dielectric permittivity and loss were measured as a function of temperature (25–300 °C), frequency (1–1000 kHz), and bias field with an Agilent E4980A LCR meter using an oscillation signal of 0.1 V. Ferroelectric hysteresis loops were measured by a Precision Premier II ferroelectric test system (Radiant Technologies).

3. Results and discussion

X-ray diffraction (XRD) patterns of the PLZT films are shown in Fig. 1. All the diffraction patterns show only well-crystallized polycrystalline perovskite phases, together with PtSi substrate, and can be well indexed by a pseudocubic structure. No other phases were detected, suggesting that neither pyrochlore phases nor interfacial reactions affected the structure. The peak position shifted toward higher angle with increasing Ti, as shown in Fig. 1(b), implying a gradual lattice distortion within the pseudocubic structure due to the variation of Zr/Ti ratios. Fig. 1(c) shows that the lattice parameter *a* decreases with increasing Ti, similar to that of bulk PLZT [23]. In the phase diagram of bulk PLZT, the

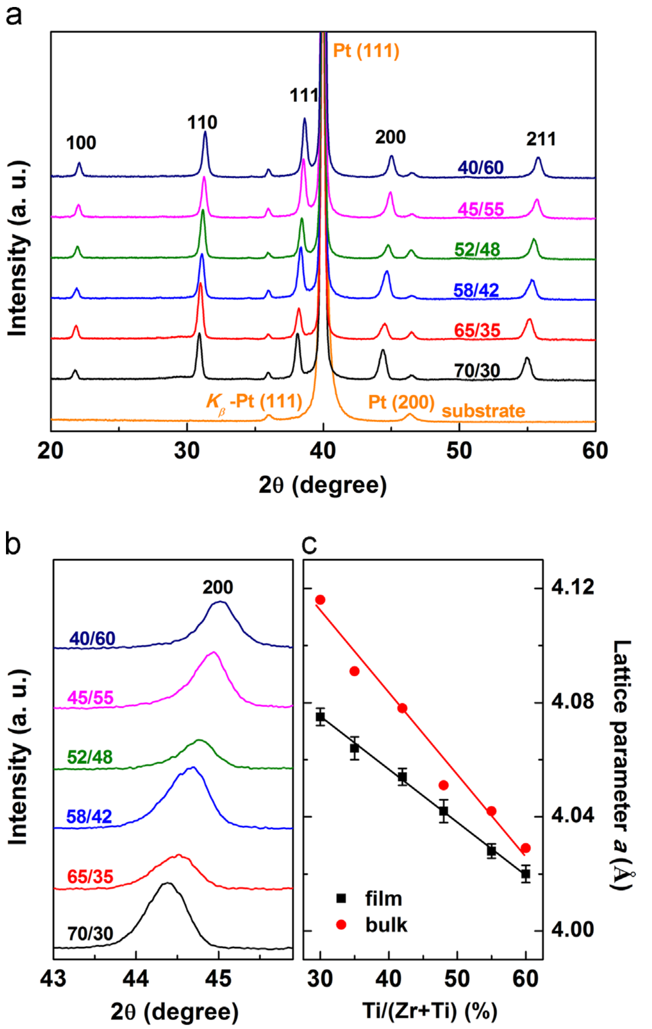

Fig. 1. (a) XRD pattern of PLZT films with different Zr/Ti ratios; (b) magnified XRD patterns in the vicinity of $2\theta = 44°$; and (c) lattice parameter *a* of PLZT films calculated from the diffraction patterns as a function of Ti content (bulk values are from Ref. [23]).

structure changes from rhombohedral to tetragonal in the vicinity of La/Zr/Ti = 8/65/35, indicated by the split of (200) peaks [5,23]. However, we did not observe such a structural transition in the XRD patterns for the PLZT films. It is known that the doping of PLZT with 8% lanthanum decreases the c\a ratio of the unit cell to near unity, resulting in a pseudocubic structure in the PLZT films, which suppresses the structural transition [2]. Another possible reason for the structural difference between the bulk and its thin film counterpart is the shift of phase boundary due to residual stress or lattice mismatch [22], similar to that previously reported in PZT films [24].

To investigate the relaxor behavior in the PLZT thin films, we measured the temperature dependence of the relative dielectric permittivity (ε_r) and dielectric loss (tan δ), as shown in Fig. 2. The broad peaks of the relative permittivity with increasing temperature are evidence of a diffuse phase transition [25,26]. The temperature for maximum permittivity, T_m, increases with increasing Ti. The dielectric loss curve being low and relatively flat in the measured temperature range indicates a low concentration of defects and high quality of all the films. For canonical relaxor ferroelectrics such as single-crystal $Pb(Mg_{1/3}Nb_{2/3})O_3$–$PbTiO_3$, the relaxor behavior is generally characterized by a strong frequency dispersion of ε_r, where T_m shifts to higher temperatures with increasing frequency. When the temperature is over T_m, ε_r is independent of frequency. For PLZT, however, these characteristics have not been generally observed, especially in thin films [12]. As previously reported, residual stresses and substrate clamping in PLZT thin films may change the order of the phase transition compared to bulk ceramic and may increase the diffuseness (broadness) of the phase transition. Therefore, it is difficult to determine the relaxor behavior directly from the temperature-dependent permittivity response [12,27,28].

To estimate the dielectric behavior of PLZT with diffuse phase transition, we used the modified Curie–Weiss law to fit the temperature-dependent dielectric permittivity [29]:

$$\frac{1}{\varepsilon_r}-\frac{1}{\varepsilon_m}=\frac{(T-T_m)^{\gamma}}{2\varepsilon_m\delta^2}\ (1\leq\gamma\leq2) \tag{1}$$

where ε_m is the maximum permittivity at T_m, δ is a shape parameter, and γ ($1\leq\gamma\leq2$) is the dispersion factor representing the degree of phase transition diffuseness. In general, $\gamma = 1$ describes the Curie–Weiss behavior of normal ferroelectrics,

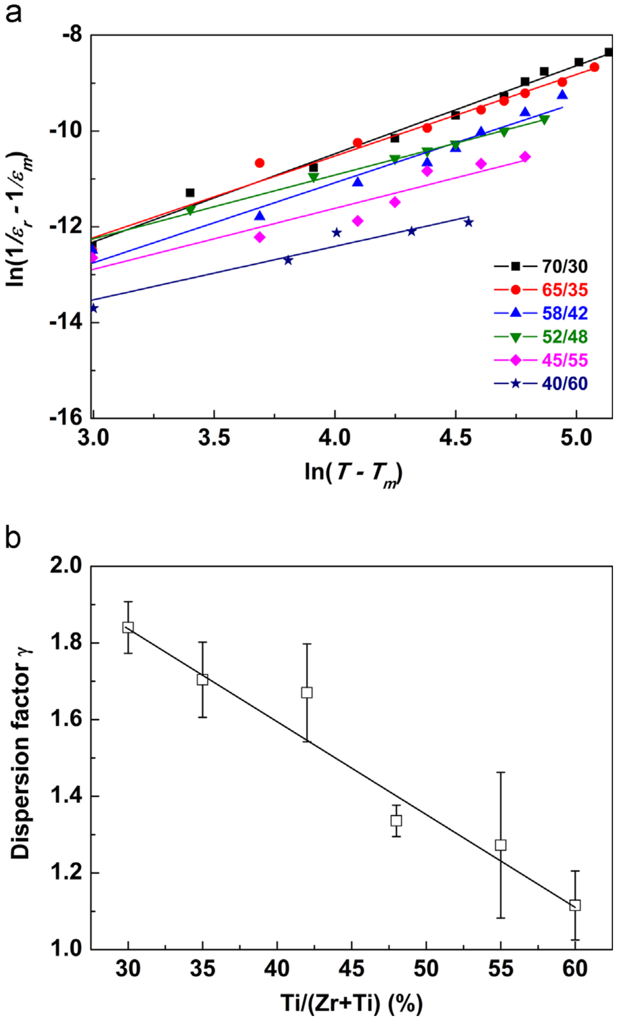

Fig. 3. (a) Fitting results of the temperature-dependent permittivity at 10 kHz using Eq. (1) and (b) dispersion factor γ as a function of Ti content.

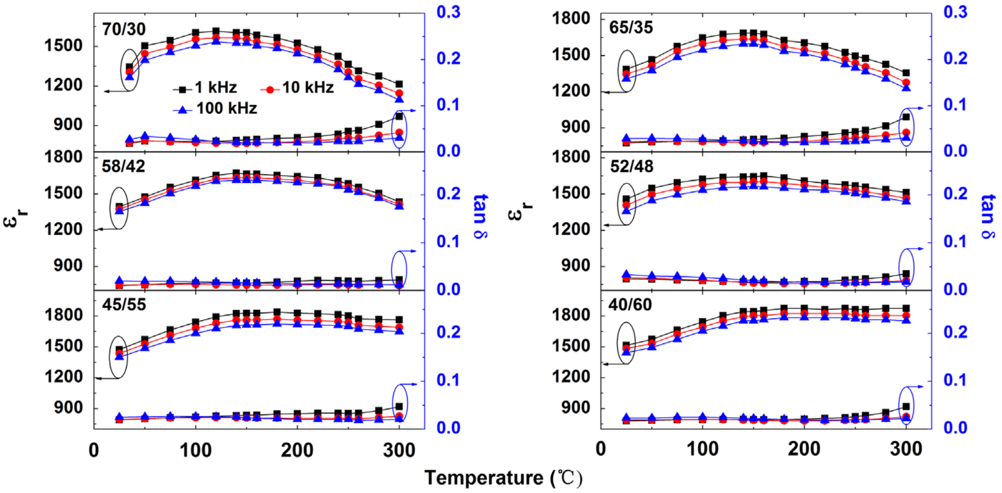

Fig. 2. Temperature-dependent relative permittivity and dielectric loss for PLZT films with different Zr/Ti ratios.

while $\gamma=2$ applies to canonical relaxor ferroelectrics that undergo a totally diffuse phase transition. The fitting results of Eq. (1) are shown as solid lines in Fig. 3(a). From the slope of the fitting lines, we can calculate the dispersion factor γ, shown in Fig. 3(b) as a function of Ti content. The dispersion factors for all the PLZT samples are lower than 2, which has been attributed to the strain and dead layer between the films and the substrates [28]. The values higher than 1 indicate that all the studied PLZT films are partially in relaxation. The dispersion factor decreases with increasing Ti content, suggesting a gradual deviation from the total relaxation state when approaching a tetragonal structure, as indicated in the phase diagram of PLZT [5].

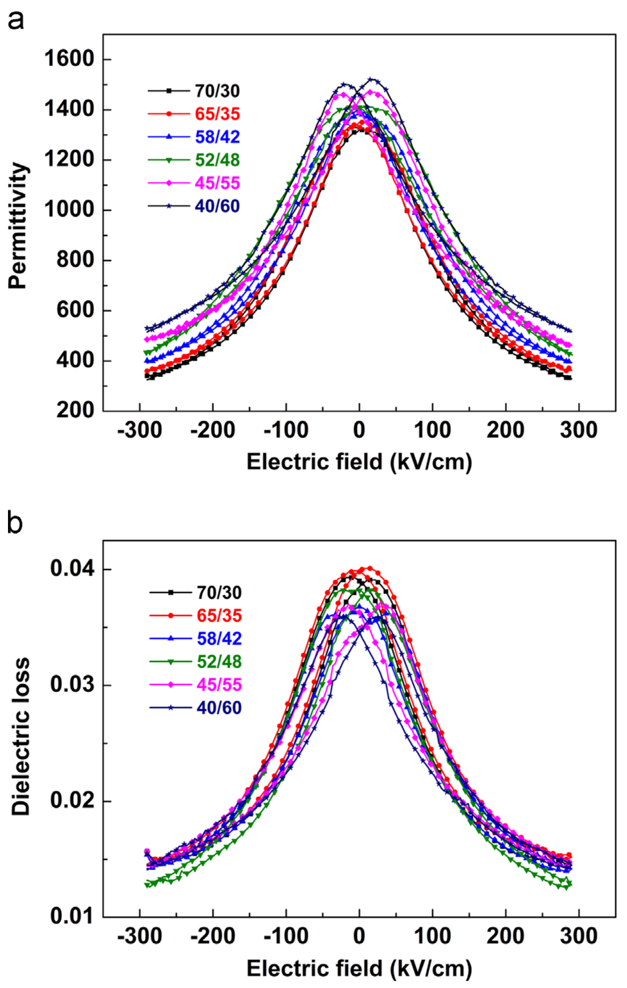

Fig. 4. (a) Relative permittivity and (b) dielectric loss as a function of electric field for the PLZT films with different Zr/Ti ratios.

Fig. 4 shows the relative permittivity and dielectric loss of the PLZT films as a function of applied bias field measured at room temperature and 10 kHz. The dielectric constant at zero bias increases with increasing Ti content, in agreement with that observed from the bulk PLZT. The dielectric tunability, defined as the ratio of change in permittivity at bias field E (200 kV/cm) and zero bias field $[1-\varepsilon(E)/\varepsilon(0)]$, decreases with increasing Ti. The dielectric losses at zero bias are in the narrow range between 0.035 and 0.04, as shown in Fig. 5. The PLZT films with Zr/Ti=52/48 exhibit a dielectric constant of ≈1400 and a dielectric loss of ≈0.038 at zero bias field. The slim butterfly-shaped curve with flat top in the PLZT 70/30 film in Fig. 4 is typical for relaxor ferroelectrics. However, the loops become relatively wide with sharp peaks at coercive electric fields, and the dielectric tunability decreases when approaching PLZT 40/60 films, indicating that a gradual transition from relaxor to normal ferroelectric occurs with increasing Ti. These observations are consistent with the aforementioned analysis of Fig. 3.

Fig. 6 shows the polarization–electric field (P–E) hysteresis loops of PLZT films measured under an electric field up to ≈725 kV/cm at a frequency of 1 kHz and room temperature. The hysteresis loops for all the samples are slim and symmetric and indicate high spontaneous polarization (P_m, ≈39–51 μC/cm^2), low remanent polarization (P_r, ≈7–13 μC/cm^2), and low coercive electric field (E_c, ≈24–34 kV/cm), which are the main features of relaxor ferroelectric PLZT films. However, P_r and E_c

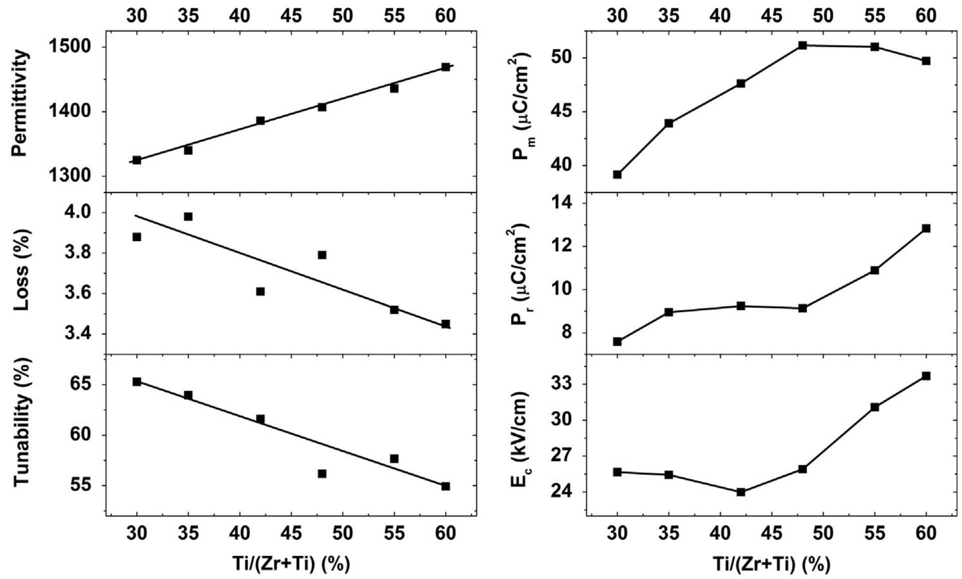

Fig. 5. Composition dependence of room-temperature ferroelectric and dielectric properties of PLZT films of various compositions.

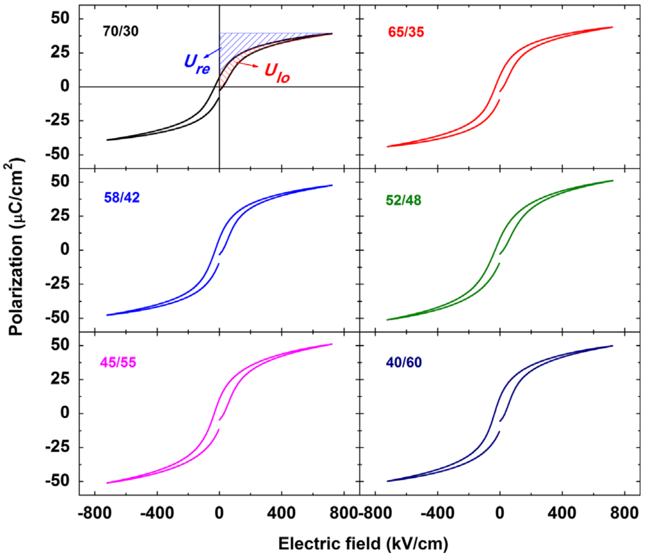

Fig. 6. *P–E* hysteresis loops of PLZT films with different Zr/Ti ratios. The shaded areas at the top left correspond to the discharged or recoverable energy density (U_{re}) and lost energy density (U_{lo}). (For interpretation of the references to color, the reader is referred to the web version of this article.).

dramatically increase in PLZT 45/55 and 40/60, approaching normal ferroelectric behavior as the dispersion factor γ decreases to lower than 1.2. The PLZT films with Zr/Ti = 52/48 exhibit the highest P_m of ≈51.2 μC/cm^2 with a relatively low P_r of ≈9.1 μC/cm^2 and a low E_c of ≈25.9 kV/cm, as shown in Fig. 5. These values are comparable to those measured on PLZT film-on-foil capacitors with the same composition [22]. The optimal electric properties of PLZT (8/52/48) films can be attributed to the shift of the morphotropic phase boundary (MPB) from 8/65/35 in the bulk material to 8/52/48 in films. This hypothesis is supported by the large tensile stress (≈250 MPa) in PLZT films deposited on PtSi [22] and a strain-induced MPB shift from Zr/Ti = 52/48 to ≈30/70 reported in PZT films [24]. However, more experimental evidence is still needed to verify this hypothesis.

We calculated the recoverable energy density (U_{re}) and the charge-discharge efficiency (η) from the *P–E* hysteresis loops of the PLZT films. In Fig. 6, U_{re} and the lost energy density U_{lo} are sketched as the blue- and red-shaded areas, respectively. As shown in Fig. 7(a), both U_{re} and η increase with increasing Ti initially, and then decrease after reaching maximum values in the films with Zr/Ti = 52/48. This decrease in both U_{re} and η can be attributed to the increase in P_r and E_c when approaching normal ferroelectric behavior. Fig. 7(b) shows the field dependences of U_{re} and η for PLZT (8/52/48) thin films. The energy density exhibits a linear increase with increasing electric field, while the energy efficiency is relatively stable when the electric field is higher than 725 kV/cm. For PLZT (8/52/48) films under an applied field of 2180 kV/cm (the maximum tested), we calculated a large energy density of ≈30 J/cm^3 with a high energy efficiency of ≈78%. These findings show that the energy storage performance of PLZT (8/52/48) is superior to that measured in relaxor polymer, ferroelectric superlattices, and PLZT (9/65/35) under the same electric field [7,8,21]. They thus suggest that PLZT (8/52/48) has potential application in high-power film capacitors.

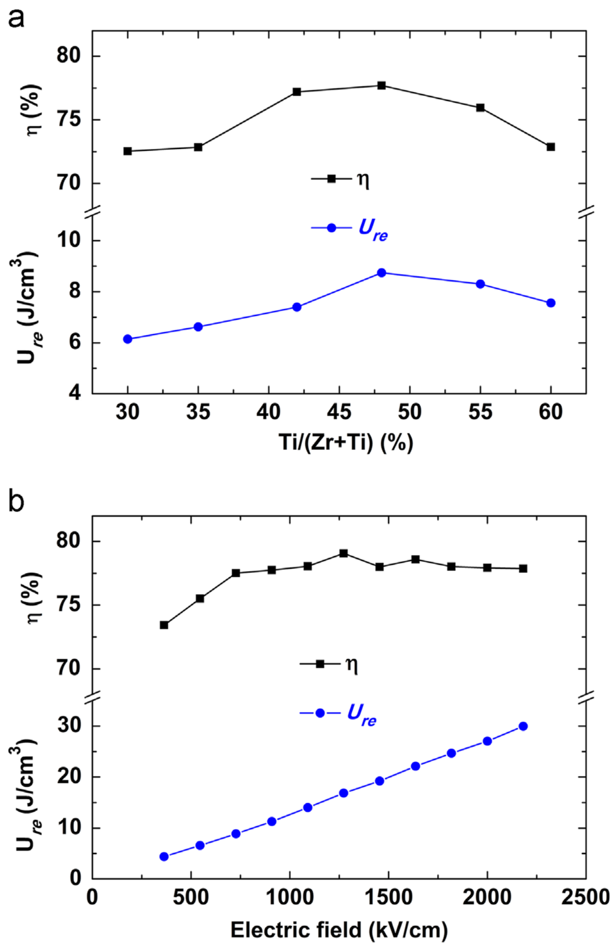

Fig. 7. (a) Composition-dependent energy density (U_{re}) and conversion efficiency (η) calculated at an applied electric field of 725 kV/cm and (b) electric field-dependent U_{re} and η of PLZT 8/52/48 thin films.

4. Conclusions

In summary, we prepared 8%-lanthanum doped PLZT films with different Zr/Ti ratios (70/30, 65/35, 58/42, 52/48, 45/55, and 40/60) on platinized silicon substrates by chemical solution deposition. XRD patterns indicated the formation of phase-pure perovskite with a pseudocubic structure in PLZT films. All the films exhibited relaxor ferroelectric behavior with diffuse phase transition. However, the degree of phase transition diffuseness decreased with increasing Ti, suggesting a gradual deviation from the total relaxation state when the tetragonal structure is approached. Typical butterfly-shaped curves for relative permittivity and loss tangent as a function of electric field and slim *P–E* loops were observed with these films. The PLZT films with Zr/Ti = 52/48 had the optimal electrical properties: a dielectric constant of ≈1400, a dielectric loss of ≈0.038, a high P_m of ≈51.2 μC/cm^2, a low P_r of ≈9.1 μC/cm^2, and a low E_c of ≈25.9 kV/cm. High energy density of ≈30 J/cm^3 and high energy efficiency of ≈78% were calculated from the *P–E* hysteresis loop of PLZT (8/52/48) films under a maximum applied field of 2180 kV/cm. These results suggest that the relaxor PLZT (8/52/48) is a promising candidate for capacitor applications, where high energy storage density and high energy efficiency are required.

Acknowledgments

This work was funded by the US Department of Energy, Vehicle Technologies Program, under Contract DE-AC02-06CH11357.

References

[1] G.R. Love, Energy storage in ceramic dielectrics, Journal of the American Ceramic Society 73 (2) (1990) 323.

[2] G.H. Haertling, Recent developments in bulk and thin film PLZT materials and devices, Ferroelectrics 131 (1) (1992) 1–12.

[3] D. Viehland, X.H. Dai, J.F. Li, Z. Xu, Effects of quenched disorder on La-modified lead zirconate titanate: long- and short-range ordered structurally incommensurate phases, and glassy polar clusters, Journal of Applied Physics 84 (1) (1998) 458–471.

[4] B. Xu, P. Moses, N.G. Pai, L.E. Cross, Charge release of lanthanum-doped lead zirconate titanate stannate antiferroelectric thin films, Applied Physics Letters 72 (5) (1998) 593.

[5] G.H. Haertling, Ferroelectric ceramics: history and technology, Journal of the American Ceramic Society 82 (4) (1999) 797–818.

[6] U. Balachandran, D.K. Kwon, M. Narayanan, B. Ma, Development of PLZT dielectrics on base metal foils for embedded capacitors, Journal of the European Ceramic Society 30 (2) (2010) 365–368.

[7] B. Chu, X. Zhou, K. Ren, B. Neese, M. Lin, Q. Wang, F. Bauer, Q.M. Zhang, A dielectric polymer with high electric energy density and fast discharge speed, Science 313 (5785) (2006) 334–336.

[8] N. Ortega, A. Kumar, J.F. Scott, D.B. Chrisey, M. Tomazawa, S. Kumari, D.G.B. Diestra, R.S. Katiyar, Relaxor-ferroelectric superlattices: high energy density capacitors, Journal of Physics: Condensed Matter 24 (44) (2012) 445901.

[9] Q. Chen, Y. Wang, X. Zhou, Q.M. Zhang, S. Zhang, High field tunneling as a limiting factor of maximum energy density in dielectric energy storage capacitors, Applied Physics Letters 92 (14) (2008) 142909.

[10] S. Tong, B. Ma, M. Narayanan, S. Liu, R. Koritala, U. Balachandran, D. Shi, Lead lanthanum zirconate titanate ceramic thin films for energy storage, ACS Applied Materials and Interfaces 5 (4) (2013) 1474–1480.

[11] H. Ogihara, C.A. Randall, S. Trolier-McKinstry, High-energy density capacitors utilizing $0.7BaTiO_3$–$0.3BiScO_3$ ceramics, Journal of the American Ceramic Society 92 (8) (2009) 1719–1724.

[12] L.E. Cross, Relaxor ferroelectrics: an overview, Ferroelectrics 151 (1) (1994) 305–320.

[13] B. Ma, S. Tong, M. Narayanan, S. Liu, S. Chao, U. Balachandran, Fabrication and dielectric property of ferroelectric PLZT films grown on metal foils, Materials Research Bulletin 46 (7) (2011) 1124–1129.

[14] M.S. Mirshekarloo, K. Yao, T. Sritharan, Large strain and high energy storage density in orthorhombic perovskite $(Pb_{0.97}La_{0.02})(Zr_{1-x-y}Sn_xTi_y)O_3$ antiferroelectric thin films, Applied Physics Letters 97 (14) (2010) 142902.

[15] J. Parui, S.B. Krupanidhi, Enhancement of charge and energy storage in sol–gel derived pure and La-modified $PbZrO_3$ thin films, Applied Physics Letters 92 (19) (2008) 192901.

[16] S. Jiang, L. Zhang, G. Zhang, S. Liu, J. Yi, X. Xiong, Y. Yu, J. He, Y. Zeng, Effect of Zr:Sn ratio in the lead lanthanum zirconate stannate titanate anti-ferroelectric ceramics on energy storage properties, Ceramics International 39 (5) (2013) 5571–5575.

[17] M. Tyunina, J. Levoska, A. Sternberg, S. Leppavuori, Relaxor behavior of pulsed laser deposited ferroelectric $(Pb_{1-x}La_x)(Zr_{0.65}Ti_{0.35})O_3$ films, Journal of Applied Physics 84 (12) (1998) 6800–6810.

[18] A. Khodorov, M. Pereira, M.J.M. Gomes, Structure and dielectric properties of sol–gel 9/65/35 PLZT thin films, Journal of the European Ceramic Society 25 (12) (2005) 2285–2288.

[19] J. Sigman, G.L. Brennecka, P.G. Clem, B.A. Tuttle, Fabrication of perovskite-based high-value integrated capacitors by chemical solution deposition, Journal of the American Ceramic Society 91 (6) (2008) 1851–1857.

[20] S.-H. Kim, C. Koo, J.-W. Lee, I.-H. Lee, W. Kim, B. Wardle, High dielectric PLZT thin films for embedded capacitors, Journal of the Korean Physics Society 54 (2009) 840.

[21] X. Hao, Y. Wang, J. Yang, S. An, J. Xu, High energy-storage performance in $Pb_{0.91}La_{0.09}(Zr_{0.65}Ti_{0.35})O_3$ relaxor ferroelectric thin films, Journal of Applied Physics 112 (11) (2012) 114111.

[22] B. Ma, S. Liu, S. Tong, M. Narayanan, U. Balachandran, Enhanced dielectric properties of $Pb_{0.92}La_{0.08}Zr_{0.52}Ti_{0.48}O_3$ films with compressive stress, Journal of Applied Physics 112 (11) (2012) 114117.

[23] G.H. Haertling, C.E. Land, Hot-pressed $(Pb,La)(Zr,Ti)O_3$ ferroelectric ceramics for electrooptic applications, Journal of the American Ceramic Society 54 (1) (1971) 1–11.

[24] Q. Yu, J.-F. Li, Z.-X. Zhu, Y. Xu, Q.-M. Wang, Shift of morphotropic phase boundary in high-performance [111]-oriented epitaxial $Pb(Zr,Ti)O_3$ thin films, Journal of Applied Physics 112 (1) (2012) 014102.

[25] A.A. Bokov, Z.-G. Ye, Dielectric relaxation in relaxor ferroelectrics, Journal of Advanced Dielectrics 02 (02) (2012) 1241010.

[26] S. Roy, P. Sarah, Dielectric properties of chemically synthesized PLZT and PZT: diffused phase transition and effect of lead non-stoichiometry, Journal of Physics D: Applied Physics 40 (15) (2007) 4668–4673.

[27] T. Kim, J.N. Hanson, A. Gruverman, A.I. Kingon, S.K. Streiffer, Ferroelectric behavior in nominally relaxor lead lanthanum zirconate titanate thin films prepared by chemical solution deposition on copper foil, Applied Physics Letters 88 (26) (2006) 262907.

[28] S. Tong, M. Narayanan, B. Ma, R.E. Koritala, S. Liu, U. Balachandran, D. Shi, Effect of dead layer and strain on the diffuse phase transition of PLZT relaxor thin films, Acta Materialia 59 (3) (2011) 1309–1316.

[29] K. Uchino, S. Nomura, Critical exponents of the dielectric constants in diffused-phase-transition crystals, Ferroelectrics 44 (1) (1982) 55–61.